Energy-momentum relation for polarons in quantum-well wires

1994 J. Phys.: Condens. Matter 6 7857

(http://iopscience.iop.org/0953-8984/6/39/007)

J. Phys.: Condens. Matter 6 (1994) 7857–7866. Printed in the UK

Energy–momentum relation for polarons in quantum-well wires

L Wendler and R Kügler

Fachbereich Physik, Martin-Luther-Universität Halle, Friedemann-Bach-Platz 6, D-06108 Halle, Germany

Received 17 May 1994, in final form 11 July 1994

Abstract. The interaction of quasi-one-dimensional electrons and longitudinal-optical (LO) phonons is calculated. Results are presented for the polaron correction to the electric subbands and the polaron effective mass. Using improved Wigner–Brillouin perturbation theory, we have investigated in detail the energy–momentum relation for quasi-one-dimensional polarons. It is shown that the dispersion curves of all subbands bend over and are pinned at the phonon continuum above the renormalized ground state. This should result in a spatial oscillation of the electron group velocity in real quantum-well wires.

1. Introduction

Advances in epitaxial layer growth and nanometre techniques have made it possible to realize *quasi-one-dimensional* (Q1D) *quantum-well wires* (QWWs) of different polar semiconductor materials. In polar semiconductors the electronic energy levels are modified by *polaronic effects* in the following manner [1, 2]: a quasi-particle, called a *polaron*, consisting of an electron and its surrounding phonon cloud, is formed. For $\alpha \ll 1$, with α the dimensionless 3D polaron coupling constant, this leads to (i) a shift in the energy: $\Delta E = -\alpha\hbar\omega_L$ with $\hbar\omega_L$ the energy of the longitudinal–optical (LO) phonon; (ii) a mass renormalization: $m_e^*/m_e = (1 - \frac{1}{6}\alpha)^{-1}$ where m_e is the effective conduction band-edge mass and m_e^* the polaron mass; (iii) a polaron-induced non-parabolicity: $\frac{3}{40}(\alpha/\hbar\omega_L)(\hbar^2k^2/2m_e)^2$ for small 3D wave vectors $k = (k_x, k_y, k_z)$; and (iv) the energy–momentum relation bends over if the polaron kinetic energy approaches the LO phonon energy above the correct ground state.

The quantum confinement of the electrons in a QWW changes these properties considerably. In 3D bulk polar semiconductors the electrons only interact with the LO phonons [3], but in layered systems of polar semiconductors the electrons interact with *modified* LO and *interface phonons* [4, 5]. Both types of phonon are also present in QWWs [6–13]. The principal difficulty in calculating the optical phonons in QWWs is that the equation of motion and the boundary conditions for the phonons do not separate in general in these geometries. This is only the case for cylindrical QWWs [7]. In the case of QWWs with rectangular cross sections mostly *ad hoc* approximations have been used. However, it was shown in [14] that such approximations lead to significant errors in the scattering rate. It was further shown in [14] that for an electron confined in a QWW with width larger than 100 nm the total scattering rate of the modified LO and interface phonons is nearly the same as that for 3D bulk LO phonons. Hence, the approximation of using 3D bulk LO phonons instead of the correct phonon spectrum provides good results for typical QWWs if the effects of the electron–phonon interaction occur as the sum over all phonon states. Further, in most QWWs the lateral confinement of the electrons is realized by an electrostatic

0953-8984/94/397857+10$19.50

potential created by a grating-type gate on top of the sample (field-effect device) and not by a structural confinement (deep-mesa etched and directly grown QWWs). In these field-effect nanostructures prepared on heterojunctions there is no influence of interfaces in the lateral direction on the spectrum of the optical phonons. Hence, Q1D polarons [15–17] and magnetopolarons [18, 19] are investigated, using the model of 3D bulk LO phonons.

In this paper we direct our attention to the energy–momentum relation for polarons, quantum confined in QWWs. The theory of the dispersion relation of 3D polarons has been given by Whitfield and Puff [20] and by Larsen [21]. Degani [22] calculated the dispersion relation of Q1D polarons in rectangular QWWs using an improved Wigner–Brillouin perturbation theory. Unfortunately the modification done in [22] to the standard form of the improved Wigner–Brillouin perturbation theory of Lindemann *et al* [23] to include the subband structure of QWWs leads to an incorrect energy–momentum relation for all excited subbands. In this paper we investigate the electron–phonon correction within second-order perturbation theory, to overcome the problems of [22]. Using the effective-mass approximation, the unperturbed system, a single electron in the presence of a confining potential acting in the y–z plane, is described by the Hamiltonian

$$H_e = p^2/2m_e + V(x) \tag{1}$$

where we assume a parabolic confining potential in the y direction, $V(x) = \frac{1}{2}m_e\Omega^2 y^2 + V(z)$, and that the electron is confined in a zero-thickness x–y plane along the z direction at $z = 0$. The eigenvalues are

$$\mathcal{E}_N(k_x) = \hbar\Omega(N + \tfrac{1}{2}) + \frac{\hbar^2 k_x^2}{2m_e} \qquad N = 0, 1, 2, \ldots \tag{2}$$

and the corresponding single-particle wavefunction is given by

$$\langle x|N, k_x\rangle = \Psi_{Nk_x}(x) = \frac{1}{\sqrt{L_x}}\exp(ik_x x)\Phi_N(y)\varphi(z) \tag{3}$$

with L_x the length of the QWW in the x direction (Born–von Kármán periodic boundary conditions), where $\Phi_N(y)$ is a harmonic oscillator wavefunction and $|\varphi(z)|^2 = \delta(z)$.

2. Electron–phonon interaction

The energy levels of an electron are shifted by the interaction of the electron with long-wavelength optical phonons. For simplicity we will assume that the electrons inside the QWW only interact with 3D bulk LO phonons.

The Hamiltonian of the polaron is $H_p = H_e + H_{ph} + H_{ep}$. The first two terms represent the unperturbed electron and the LO phonon system and H_{ep} is the standard Fröhlich Hamiltonian of the electron–phonon interaction [3]:

$$H_{ph} = \sum_q \hbar\omega_L(a_L^+(q)a_L(q) + \tfrac{1}{2}) \tag{4}$$

and

$$H_{ep} = \left(\frac{4\pi\alpha r_p(\hbar\omega_L)^2}{V_G}\right)^{1/2}\sum_q e^{iq\cdot x}\frac{1}{|q|}(a_L(q) + a_L^+(-q)) \tag{5}$$

with

$$\alpha = \frac{1}{2}\frac{e^2}{4\pi\epsilon_0 r_p}\left(\frac{1}{\epsilon_\infty} - \frac{1}{\epsilon_s}\right)\frac{1}{\hbar\omega_L}$$

the dimensionless 3D polaron coupling constant and $r_p = (\hbar/2m_e\omega_L)^{1/2}$ the corresponding 3D polaron radius. ϵ_∞ and ϵ_s are the high-frequency (optical) and the static dielectric constant of the semiconductor containing the electron, respectively, and ϵ_0 is the permittivity of vacuum. Further, $a_L(q)$ and $a_L^+(-q)$ are the phonon destruction and creation operators and q is the 3D wave vector of the LO phonons.

In the weak-coupling limit ($\alpha \ll 1$), valid for typical semiconductor materials forming QWWs, second-order perturbation theory can be used. Then the energy shift $\Delta E_N(k_x)$ of the subband energy $E_N(k_x) = \mathcal{E}_N(k_x) + \Delta E_N(k_x)$ is given by

$$\Delta E_N(k_x) = -\sum_{N'=0}^{\infty} \sum_{q} \frac{|M_{N'N}(q)|^2}{D_{N'N}(k_x, q_x)} \tag{6}$$

where $M_{N'N}(q) = \langle N', k_x - q_x; 1_q | H_{ep} | N, k_x; 0_q \rangle$ is the corresponding matrix element. The ket $|N, k_x; n_q\rangle = |N, k_x\rangle \otimes |n_q\rangle$ describes an eigenstate of $H_0 = H_e + H_{ph}$ composed of an electron in subband N with momentum $\hbar k_x$ and n_q LO phonons with momentum $\hbar q$ and energy $\hbar\omega_L$. The corresponding level we call the *n-phonon unperturbed level*, as opposed to the renormalized level, the *n-phonon polaron level*. The energy denominator in equation (6) is given by

$$D_{N'N}(k_x, q_x) = \hbar\omega_L + \hbar\Omega(N' - N) + \frac{\hbar^2 q_x^2}{2m} - \frac{\hbar^2}{m} k_x q_x - \Delta_N(k_x) \tag{7}$$

where the value of $\Delta_N(k_x)$ depends on the type of perturbation theory used [23]: (i) $\Delta_N(k_x) = 0$ leads to *Rayleigh–Schrödinger perturbation theory* (RSPT), (ii) $\Delta_N(k_x) = \Delta E_N(k_x)$ results in the *Wigner–Brillouin perturbation theory* (WBPT) and (iii) $\Delta_N(k_x) = \Delta E_N(k_x) - \Delta E_0^{RSPT}(0)$ gives a *modified* improved Wigner–Brillouin perturbation theory (IWBPT, for details see below), with $\Delta E_0^{RSPT}(0)$ the electron–phonon correction to the electron ground-state energy calculated within RSPT. Introducing in equation (6) 3D polaron units (energies are measured in units of $\hbar\omega_L$ and lengths are in units of r_p) and converting the sum over the phonon momentum into an integral, one gets

$$\Delta E_N(k_x) = -\frac{\alpha}{2\pi} \int_0^\infty dq_\parallel \int_{-\pi}^{\pi} d\varphi\, e^{-a} \sum_{N'=0}^{\infty} \frac{N_2!}{N_1!}\, a^{N_1 - N_2} \times \frac{[L_{N_2}^{N_1-N_2}(a)]^2}{1 + \eta(N' - N) + q_\parallel^2 \cos^2\varphi - 2k_x q_\parallel \cos\varphi - \Delta_N(k_x)} \tag{8}$$

with $a = q_\parallel^2 \sin^2\varphi/\eta$ and $N_1 = \max(N, N')$ and $N_2 = \min(N, N')$, $q_\parallel = |q_\parallel| = (q_x^2 + q_y^2)^{1/2}$, $\eta = \Omega/\omega_L$ and where we have introduced cylindrical coordinates in the q_x–q_y plane; $L_N^{N'}(\xi)$ is the associated Laguerre polynomial. This expression can be expanded in powers of k_x^2: $\Delta E_N(k_x) = \Delta E_N(0) + \Delta E_N'(0) k_x^2 + \frac{1}{2}\Delta E_N''(0) k_x^4 + \ldots$ and so the polaron effective mass m_N^* for the polaron motion in the x direction near the bottom of the subband $E_N(k_x)$ is

$$\frac{m_N^*}{m_e} = \frac{1}{1 + (2m_e/\hbar^2)\Delta E'(0)}. \tag{9}$$

Note that WBPT and IWBPT make equation (8) self-consistent with the result that higher powers of α in $\Delta E_N(k_x)$ and m_N^* occur. Considering for the moment the energy–momentum relation for the n-phonon unperturbed states, it is obvious that below the one-phonon energy $\mathcal{E}_0(0) + \hbar\omega_L$ there is only a finite number of subbands, i.e. from zero-phonon states. Above $\mathcal{E}_0(0) + \hbar\omega_L$ there is a continuum of states, called the *phonon continuum*, for each value

of the polaron momentum. The electron–phonon interaction couples the degenerate states, leading to a splitting of a zero-phonon state into an upper and a lower branch. The upper branch is above the boundary of the phonon continuum, but the lower branch is below this line. Hence, all states $|N, k_x; 0_q\rangle$ lying below the energy $\mathcal{E}_0(0) + \hbar\omega_L$ must bend over if their energies approach the near vicinity of the boundary of the phonon continuum because of the anticrossing repulsion. For larger momenta these states are then pinned at this line. In this picture the bend-over starts at $k_x^{(N)} = \sqrt{2m_e/\hbar(\omega_L - N\Omega)}$ for subband N. Because the electron–phonon interaction renormalizes the energies to $E_N(k_x) = \mathcal{E}_N(k_x) + \Delta E_N(k_x)$, the accurate dispersion curves of all subbands must bend over at $E_0(0) + \hbar\omega_L$, i.e. the one-phonon energy $\hbar\omega_L$ above the *shifted* ground state $E_0(0) = \mathcal{E}_0(0) + \Delta E_0(0)$ of the system. For further consideration only the lower branches below the phonon continuum are of interest.

The RSPT describes the energy correction $\Delta E_N(k_x)$ quite well if $k_x \ll k_x^{(N)}$, but it fails near $k_x^{(N)}$. The energy shift $\Delta E_N(k_x)$ calculated using non-degenerate RSPT diverges negatively (near but below) at $k_x^{(N)}$ for any strength of the coupling because the energy denominator in equation (8) vanishes at $k_x^{(N)}$. Hence, degenerate perturbation theory has to be used. One possibility is to use WBPT. But unfortunately WBPT gives a bend-over at $\mathcal{E}_0(0) + \hbar\omega_L$, the one-phonon energy above the unperturbed ground state $\mathcal{E}_0(0)$, which would lead to the wrong result that the polarons in the bend-over region could decay into a phonon and an electron. In order to get the dispersion relation $E_N(k_x)$ of each subband with the correct bending-over and pinning behaviour IWBPT must be used. Modifying the IWBPT of Lindemann *et al* [23] to the case of polarons in QWWs we start from the unperturbed energy $\mathcal{E}_N(k_x) + \Delta E_0^{\mathrm{RSPT}}(0)$ and take this level as the reference level for the excited states by decomposing H_p as $H_p = (H_0 + \Delta E_0^{\mathrm{RSPT}}(0)) + (H_{ep} - \Delta E_0^{\mathrm{RSPT}}(0))$. This results in equation (7) with $\Delta_N(k_x) = \Delta E_N(k_x) - \Delta E_0^{\mathrm{RSPT}}(0)$. It is seen later that this modification of the IWBPT gives the correct bending-over and pinning for all subbands. In contrast to our modification, Degani [22] uses $\Delta_N(k_x) = \Delta E_N(k_x) - \Delta E_N^{\mathrm{IWBPT}}(0)$ with the wrong result that the higher levels bend over at $\mathcal{E}_0(0) + \Delta E_N^{\mathrm{IWBPT}}(0) + \hbar\omega_L$, which is different for different subbands.

We note that for unperturbed states with $\omega_L < N\Omega$ the corresponding bottoms of the electric subbands are inside the phonon continuum. Here, we only consider the QID polaron dispersion relation below the phonon continuum. To analyse the QID polaron energy–momentum relation in detail we calculate the energy corrections $\Delta E_0(k_x)$ and $\Delta E_1(k_x)$ of the two lowest subbands. For the calculation of the energy shifts we convert the denominator in equation (8) by the integral

$$\frac{1}{D_{N'N}(k_x, q_x)} = \int_0^\infty \mathrm{d}t\ \exp[-D_{N'N}(k_x, q_x)t] \tag{10}$$

which is possible under the condition $D_{N'N}(k_x, q_x) > 0$, restricting the calculation to energies below the phonon continuum and obtain for the two lowest subbands

$$\Delta E_N(k_x) = -\frac{\alpha}{\sqrt{\pi}} \int_0^\infty \mathrm{d}t\ \exp(-(1 - \Delta_N(k_x))t) \times \int_0^{\pi/2} \mathrm{d}\varphi \exp\left(\frac{tk_x^2 \cos^2\varphi}{1 - A(t)\sin^2\varphi}\right) [(1 - A(t)\sin^2\varphi)t]^{-1/2} \Lambda_0^N(t) \tag{11}$$

with $A(t) = (\mathrm{e}^{-\eta t} - 1 + \eta t)/\eta t$, $\Lambda_0^0(t) = 1$ and

$$\Lambda_0^1(t) = \left\{1 + 2\frac{(\cosh \eta t - 1)\ \sin^2\varphi}{(1 - A(t)\sin^2\varphi)\ \eta t}\right\}.$$

Performing in equation (11) the integral over the angle, we obtain for the renormalization of the first two states

$$\Delta E_N(0) = -\frac{\alpha}{\sqrt{\pi}} \int_0^\infty \mathrm{d}t \, \frac{\exp(-(1-\Delta_N(0))t)}{\sqrt{t}} \, \Lambda_1^N(t) \tag{12}$$

with $\Lambda_1^0(t) = \boldsymbol{K}[A(t)]$ and

$$\Lambda_1^1(t) = \left\{ \boldsymbol{K}[A(t)] + 2\frac{\cosh \eta t - 1}{A(t)^2 \, \eta t} \left(\frac{\boldsymbol{E}[A(t)]}{A'(t)^2} - \boldsymbol{K}[A(t)] \right) \right\}.$$

The corresponding derivatives are given by

$$\left. \frac{\mathrm{d}}{\mathrm{d}(k_x^2)} \Delta E_N(k_x) \right|_{k_x=0} = -\frac{\alpha}{\sqrt{\pi}} \int_0^\infty \mathrm{d}t \, \frac{\exp(-(1-\Delta_N(0))t)}{(1-\Delta_N'(0))} \, \sqrt{t} \, \Lambda_2^N(t) \tag{13}$$

with $\Lambda_2^0(t) = \boldsymbol{D}[A(t)]$,

$$\Lambda_2^1(t) = \left\{ \boldsymbol{D}[A(t)] + 2\frac{\cosh \eta t - 1}{A(t)^2 \, \eta t} \left(\frac{\boldsymbol{E}[A(t)]}{A'(t)^2} - 2\boldsymbol{D}[A(t)] \right) \right\}$$

$\Delta_N'(0) = 0$ in RSPT and $\Delta_N'(0) = \Delta E_N(0)$ in WBPT and IWBPT. $\boldsymbol{K}(\xi)$ is the complete elliptical integral of the first kind, $\boldsymbol{E}(\xi)$ the complete elliptical integral of the second kind and $\boldsymbol{D}(\xi)$ that of the third kind. $A'(t) = \sqrt{1 - A(t)^2}$ is the complementary modulus of the elliptical integrals.

3. Discussion

For numerical calculation we have used a GaAs–$Ga_{1-x}Al_xAs$ QWW (GaAs: $\alpha = 0.07$, $r_p = 3.987$ nm, $\hbar\omega_L = 36.17$ meV, $m_e = 0.06624m_0$, m_0: bare electron mass) where the electrons are confined within GaAs.

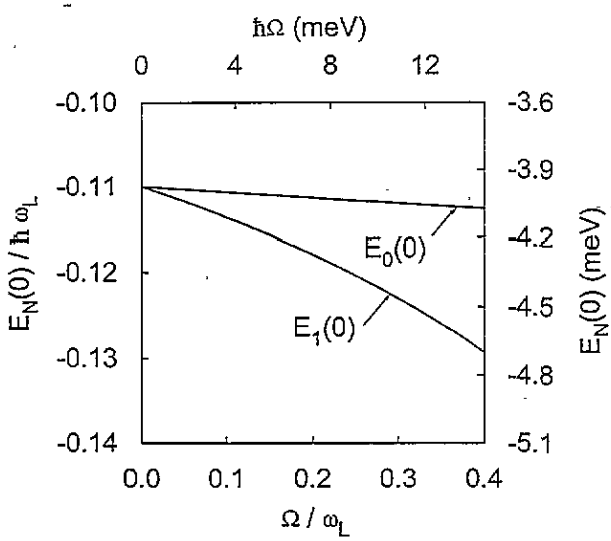

Figure 1. Polaronic energy renormalization of the first two electric subbands for a GaAs–$Ga_{1-x}Al_xAs$ QWW as a function of the confinement energy.

The calculated zero-momentum energy renormalizations of the two lowest subbands are plotted in figure 1. It is seen that with increasing confinement the polaronic renormalization

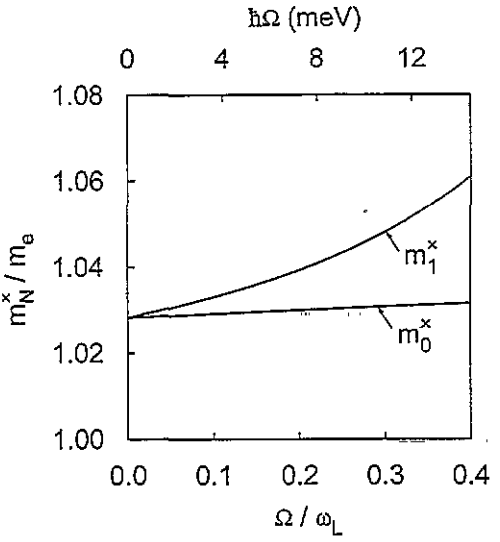

Figure 2. Polaron effective mass of the two lowest electric subbands for a GaAs–$Ga_{1-x}Al_xAs$ QWW as a function of the confinement energy.

increases more for $\Delta E_1(0)$ than for $\Delta E_0(0)$. For vanishing geometrical confinement frequency Ω we obtain from equation (12) in the lowest order of α the well known result for 2D polarons $\Delta E_0(0) = \Delta E_1(0) = -\frac{1}{2}\pi\alpha$. The polaron masses are plotted in figure 2. It is seen that the polaron mass of the lowest subband m_0^* depends on the confinement much more weakly than the polaron mass m_1^* of the first excited subband. For vanishing confinement potential we obtain from equation (13) $m_0^*/m_e = m_1^*/m_e = (1 - \alpha\pi/8)^{-1}$. In figure 3 the polaron dispersion curves of the lowest subband are plotted, $E_0(k_x)$, calculated with RSPT, WBPT and IWBPT. It is seen that for a polaron wave vector $k_x \ll k_x^{(0)}$ the three perturbation theories give nearly the same result. In RSPT the energy $E_0(k_x)$ diverges negatively at $k_x^{(0)}$ and fails to describe the correct polaron energy–momentum relation for all momenta. Further, WBPT results in the wrong bend-over behaviour at the boundary of the unrenormalized phonon continuum. The IWBPT shows the correct bend-over and pinning behaviour at the boundary of the renormalized phonon continuum. As in the 3D and 2D cases the dispersion relation is essentially parabolic for small momentum but becomes strongly non-parabolic in the near vicinity of $k_x^{(0)}$.

In figure 4 the IWBPT Q1D polaron energy–momentum relation is plotted in the bend-over region for different confining potentials. It is seen that the anticrossing repulsion between the zero-phonon renormalized state and the renormalized phonon continuum increases with increasing frequency of the confining potential, i.e. with narrowing of the width of the Q1D channel. The dispersion curves $E_0(k_x)$ and $E_1(k_x)$ of the two lowest subbands are plotted in figure 5. These curves are calculated with IWBPT. From this figure it is seen that both dispersion curves are pinned at the boundary of the renormalized phonon continuum. Hence, the modification of the IWBPT, developed in this paper, gives the correct bending-over and pinning behaviour for higher states also. Therefore we have overcome the problems with the form of the IWBPT developed in [22] resulting in the incorrect bend-over and pinning behaviour for higher subbands.

Figure 6 shows the group velocity

$$v_N = \frac{1}{\hbar}\frac{\mathrm{d}E_N}{\mathrm{d}k_x}$$

for Q1D polarons of the two lowest subbands. The polaron moving in the x direction under the influence of a weak electric field accelerates until the polaron wave vector reaches $k_x^{(N)}$,

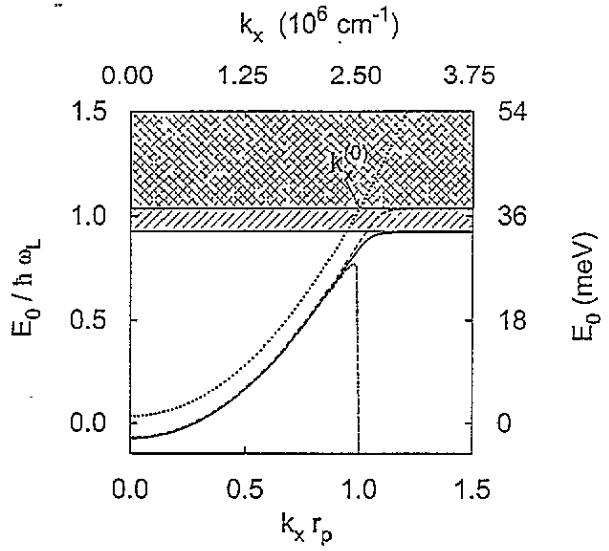

Figure 3. Energy–momentum relation for QID polarons in the lowest subband of a GaAs–$Ga_{1-x}Al_xAs$ QWW with $\hbar\Omega$ = 2.5 meV. The results are plotted for IWBPT (full curve), WBPT (broken curve) and RSPT (chain curve). The corresponding unperturbed energy–momentum relation is plotted as a dotted curve. The unrenormalized phonon continuum is plotted as the crossed shaded area and the renormalized phonon continuum as the single shaded area.

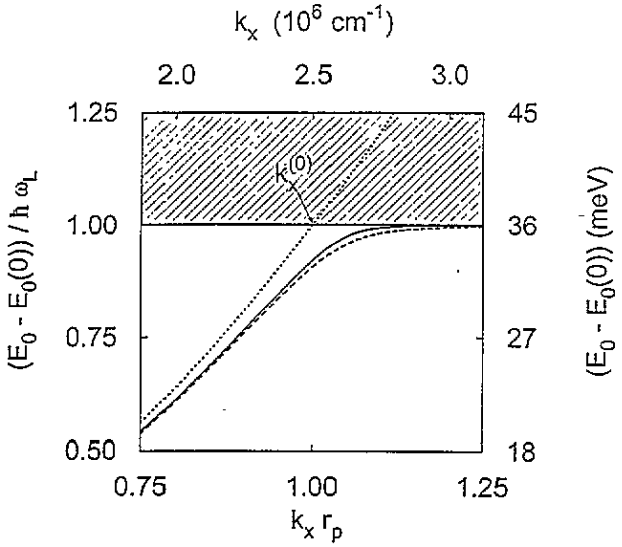

Figure 4. Energy–momentum relation for QID polarons in the lowest subband of a GaAs–$Ga_{1-x}Al_xAs$ QWW calculated using IWBPT. The results are plotted for $\hbar\Omega$ = 2.5 meV (full curve) and for $\hbar\Omega$ = 12 meV (broken curve). The corresponding unperturbed energy–momentum relation is plotted as a dotted curve. The single shaded area is the renormalized phonon continuum.

whereupon it slows down sharply. The reason for this behaviour is that the electron–phonon interaction induces a negative effective mass in the bend-over region. Increasing polaron momentum will slow down the velocity and stop the propagation until it can gain energy to either emit a real phonon or transfer to the upper branch inside the phonon continuum. Since the energy gap to emit a real phonon is smaller than the gap between the two resonance split branches, the probability for the LO phonon emission process is enhanced in comparison to the transfer to the upper branch. The polaron cannot emit a real phonon, because there is a finite energy difference between $E_N(k_x)$ and the boundary of the renormalized phonon continuum. In real systems, however, the energy levels are broadened due to scattering processes. The energy broadening $\Gamma = \hbar/\tau_e$ ($\tau_e = m_e\mu/e$: elastic scattering time; μ: electron mobility) is typically between 1×10^{-3} and 5×10^{-2} meV in semiconductor nanostructures based on GaAs–$Ga_{1-x}Al_xAs$ heterostructures. Then it is possible that the

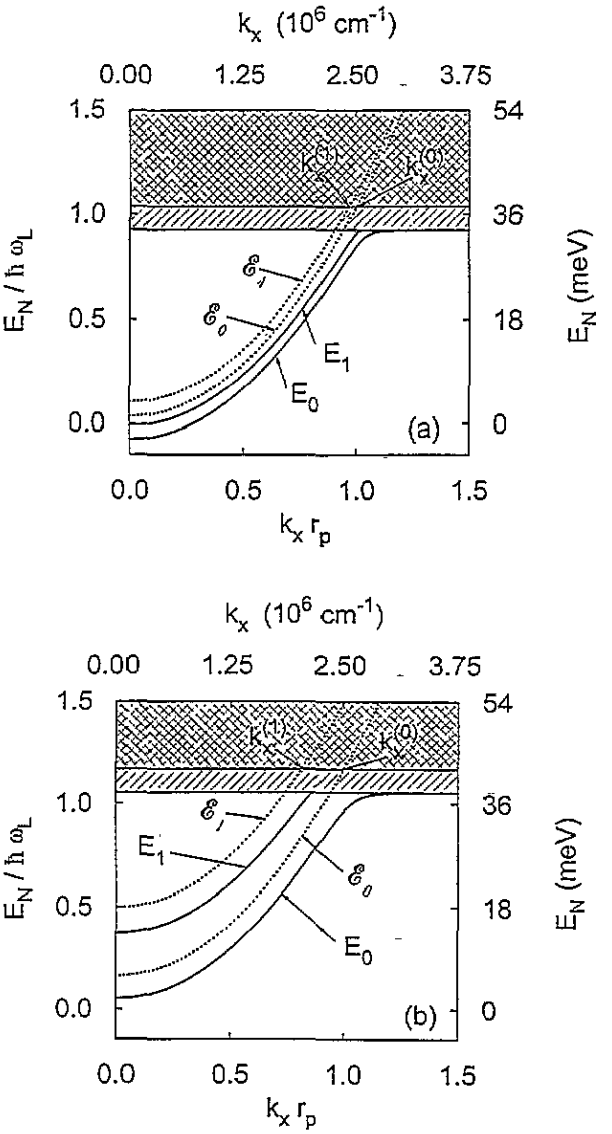

Figure 5. Energy–momentum relation for QID polarons in the two lowest subbands of a GaAs–$Ga_{1-x}Al_xAs$ QWW with $\hbar\Omega$ = 2.5 meV (a) and $\hbar\Omega$ = 12 meV (b) *calculated using* IWBPT. The corresponding unperturbed energy–momentum relations $\mathcal{E}_0(k_x)$ and $\mathcal{E}_1(k_x)$ are plotted as dotted curves. The unrenormalized phonon continuum is plotted as the crossed shaded area and the renormalized phonon continuum as the single shaded area.

polaron emits a real phonon if the energy is large enough. After emitting a real phonon the polaron relaxes to the subband minimum, where the electric field again accelerates the polaron. This effect should be observable in transport experiments on QWWs. It is expected that the electron velocity shows spatial oscillations dependent on the strength of the applied electric field. In a real QWW the electrons become scattered, not only by the optical phonons, but also by the residual impurities and by acoustic phonons via both the deformation potential and the piezoelectric mechanism. While the impurity scattering is elastic, the scattering by acoustic phonons is inelastic and hence leads to dephasing of the electron transport. The result is that the oscillations of the electron velocity should persist for several periods until spatial dephasing by the interaction with the acoustic phonons. Only for long QWWs at low temperatures and for low external electric fields is the transport dominated by electron–acoustic phonon scattering which causes a rapid dephasing and randomization before the electrons are allowed to drift up to the LO phonon emission threshold. For higher

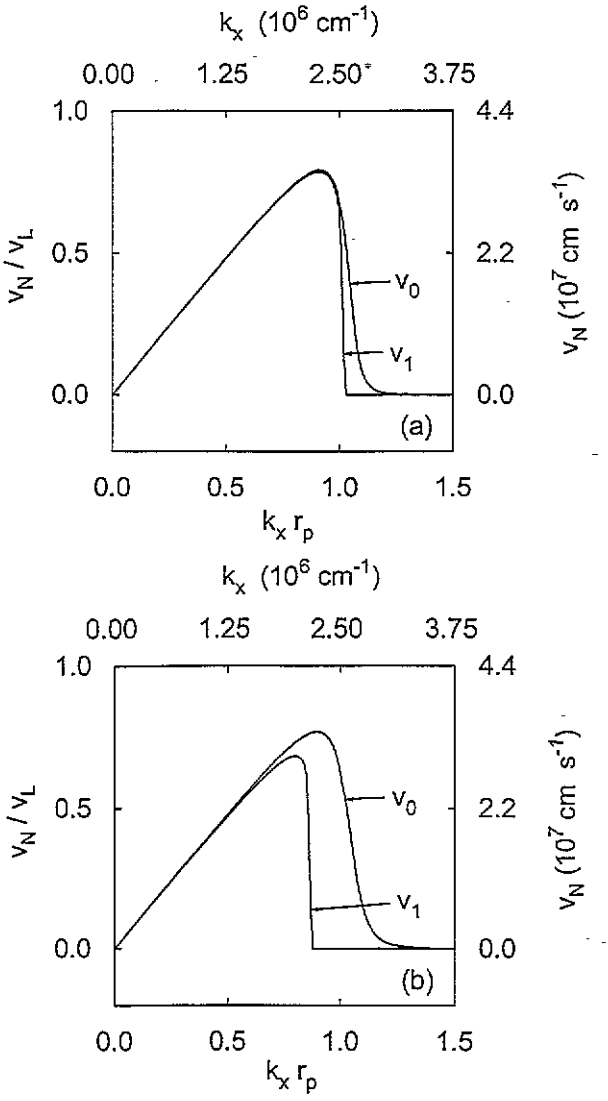

Figure 6. Polaron group velocity plotted against polaron wave vector for propagation in the two lowest subbands of a GaAs–$Ga_{1-x}Al_xAs$ QWW with $\hbar\Omega =$ 2.5 meV (a) and $\hbar\Omega = 12$ meV (b) calculated using IWBPT. $v_L = 2r_p\omega_L = 4.38 \times 10^7$ cm s^{-1} is the unperturbed electron group velocity at $k_x^{(0)} = 1/r_p$.

fields the carrier transport will be essentially ballistic up to the LO phonon threshold and, hence, electron velocity oscillations should occur in real QWWs. Similar findings have been reported recently [24] using 1D Monte Carlo simulations of electron transport through QWWs.

4. Conclusions

We have presented the calculation of the dispersion relation for polarons quantum confined in Q1D QWWs. The developed theory modifies the IWBPT and gives the correct bend-over and pinning behaviour of the dispersion curves for all subbands at the boundary of the renormalized phonon continuum. This boundary is at the one-phonon energy above the shifted ground state $\mathcal{E}_0(0) + \Delta E_0(0) + \hbar\omega_L$ of the system due to electron–phonon interaction. Our theory is valid for zero temperature and momenta for which the effective-mass approximation is valid. It overcomes the problems of the theory of Degani [22] to give the correct dispersion curves for the higher subbands also. Further, the results obtained here are in agreement with that of Hellman and Harris [25, 26]. In this work the

energy–momentum relation is investigated for 3D polarons travelling along the direction of an applied magnetic field, using a variational calculation. There are some similarities to the case of the QWW considered here, because the magnetic field quantizes the electron motion in the perpendicular plane. The variational principle, however, only allows the calculation of the ground-state energy, in contrast to the modified IWBPT developed in this paper.

Throughout this paper we have only considered the interaction with 3D bulk LO phonons, because the effect of the modification of the spectrum of the long-wavelength optical phonons due to the interfaces is expected to be small. The modified LO phonons are standing waves inside the QWW with energy $\hbar\omega_L$. Hence, this will not shift the phonon continuum. The interface phonons have a dispersion curve $\omega(q_x)$ lying below the LO phonon frequency. Hence, the interaction of the electron with the interface phonons of QWWs will shift the phonon continuum to lower frequencies. Further possible improvements on these results would be the inclusion of the conduction-band non-parabolicity (the band structure effect), the non-parabolicity of the confining potential, the finite width of the QWW in the growth direction and, if many electrons are present, occupation and screening effects. Special attention must be directed to higher electric subbands with bottoms above the threshold of the phonon continuum.

Acknowledgment

We would like to thank R Haupt for useful discussions.

References

[1] Kuper G and Whitfield G (ed) 1963 *Polarons and Excitons* (Edinburgh: Oliver and Boyd)
[2] Devreese J T (ed) 1972 *Polarons in Ionic Crystals and Polar Semiconductors* (Amsterdam: North-Holland)
[3] Fröhlich H 1954 *Adv. Phys.* **3** 325
[4] Wendler L 1985 *Phys. Status Solidi* b **129** 513
[5] Haupt R and Wendler L 1991 *Phys. Rev.* B **44** 1850
[6] Stroscio M A 1989 *Phys. Rev.* B **40** 6428
[7] Constantinou N C and Ridley B K 1990 *Phys. Rev.* B **41** 10627
[8] Stroscio M A, Kim K W, Littlejohn M A and Chuang H 1990 *Phys. Rev.* B **42** 1488
[9] Zhu K-D and Gu S-W 1992 *J. Phys.: Condens. Matter* **4** 1291
[10] Knipp D A and Reinecke T L 1992 *Phys. Rev.* B **45** 9091
[11] Campos V B, Das Sarma S and Stroscio M A 1992 *Phys. Rev.* B **46** 3849
[12] Mickevičius R, Mitin V V, Kim K W, Stroscio M A and Iafrate G J 1992 *J. Phys.: Condens. Matter* **4** 4959
[13] Li W S, Gu S-W, Au-Yeung T C and Yeung Y Y 1992 *Phys. Rev* B **46** 4630
[14] Knipp D A and Reinecke T L 1993 *Proc. 6th Int. Conf. on Modulated Semiconductor Structures (Garmisch-Partenkirchen)* p 783
[15] Degani M H and Hipólito O 1987 *Phys. Rev.* B **35** 9345
[16] Degani M H and Hipólito O 1988 *Solid State Commun.* **65** 1185
[17] Hai G Q, Peeters F M, Devreese J T and Wendler L 1993 *Phys. Rev.* B **48** 12016
[18] Zhou H Y, Zhu K-D and Gu S-W 1992 *J. Phys.: Condens. Matter* **4** 4613
[19] Wendler L, Chaplik A V, Haupt R and Hipólito O 1993 *J. Phys.: Condens. Matter* **5** 4817
[20] Whitfield G and Puff R 1965 *Phys. Rev.* **139** A338
[21] Larsen D M 1966 *Phys. Rev.* **144** 697
[22] Degani M H 1989 *Phys. Rev.* B **40** 11937
[23] Lindemann G, Lassnig R, Seidenbusch W and Gornik E 1983 *Phys. Rev.* B **28** 4693
[24] Jovanovic D and Leburton J P 1992 *Superlatt. Microstruct.* **11** 2
[25] Hellman E and Harris J S 1986 *Surf. Sci.* **174** 459
[26] Hellman E and Harris J S 1986 *Phys. Rev.* B **33** 8284